

# Level 1 jet trigger simulations for the ALICE Electromagnetic Calorimeter

André Mischke (Utrecht University, LBNL)\*  
and Peter Jacobs (CERN, LBNL)†

August 16, 2005

## 1 Introduction

Medium-induced modification of jet fragmentation (“jet quenching”) is a sensitive and far-reaching probe of the matter created in high energy nuclear collisions at RHIC [1]. Jet studies will play a central role in the LHC heavy ion program, but the baseline ALICE detector has limited capability in this direction. It has long been recognized that an electromagnetic calorimeter (EMCal) would add significant physics capabilities to ALICE, in particular for jet triggering and measurement, and an EMCal proposal is under development (for a recent update see [2]). The proposed EMCal has a sampling Pb/scintillator structure (1.5 mm/1.5 mm,  $\sim 80$  layers,  $\sim 22$  radiation lengths) with shashlik-type wavelength shifting fiber geometry. The fibers are read out by Avalanche Photodiodes. The nominal resolution for this choice of absorber and scintillator thicknesses is  $\sigma_E/E \sim 8\%/\sqrt{E}$ . The nominal acceptance is  $0 < \Delta\phi < 2\pi/3, |\Delta\eta| < 0.7$ , comprising  $\sim 15k$   $\eta$ -projective towers.

Full exploitation jets as a probe of dense matter at the LHC will require the study of the evolution of jet fragmentation over a broad jet energy range, from the moderate energy jets studied at RHIC where quenching effects are seen to be strong, to jets with energies well beyond 100 GeV where quenching effects are expected to be negligible. Annual yields for various hard processes in ALICE for minimum bias Pb+Pb at nominal luminosity ( $L = 5 \times 10^{26} \text{cm}^{-2} \text{s}^{-1} \times 10^6 \text{s} = 0.5 \text{nb}^{-1}$ ) are shown in Fig. 1. Within the EMCal acceptance the annual jet yields are large:  $10^7$  per year for  $E_T > 50$  GeV ( $\sim 10$  Hz) and  $4 \times 10^5$  per year for  $E_T > 100$  GeV. Due to the finite EMCal acceptance the yield is reduced by a factor  $\sim 2$  for a jet patch trigger of dimensions  $\Delta\eta \times \Delta\phi = 0.4 \times 0.4$  (see vertical arrows on Fig. 1), dimensions which are on the large side for a jet definition in heavy ion collisions.

Minimum bias events at nominal luminosity occur at 4-8 kHz but can be recorded by ALICE only at  $\sim 100$  Hz. A Level 1 (L1) trigger is therefore required in Pb+Pb collisions to take advantage of the large jet yields. The EMCal provides such a jet trigger on the L1 time scale of  $\sim 6\mu\text{s}$ , though with a potential bias since it is sensitive largely to the electromagnetic energy in the jet.

---

\*a.mischke@phys.uu.nl

†pmjacobs@lbl.gov

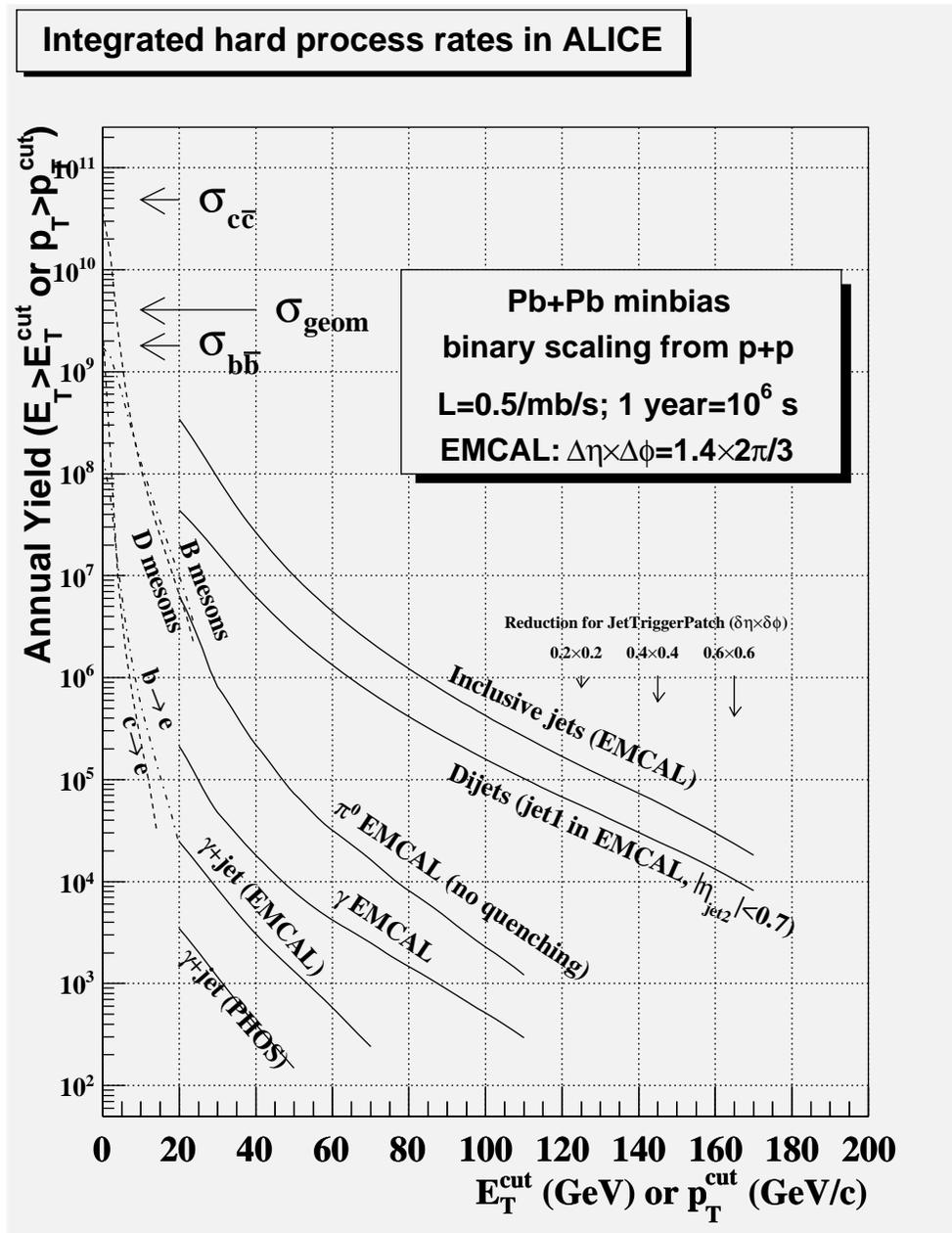


Figure 1: Hard process annual yields ( $10^6$  seconds) in ALICE acceptance for minbias Pb+Pb at nominal luminosity. Calculations derived from [3, 4, 5, 6]. Vertical arrows indicate yield reduction due to EMCAL acceptance for various jet trigger patch sizes.

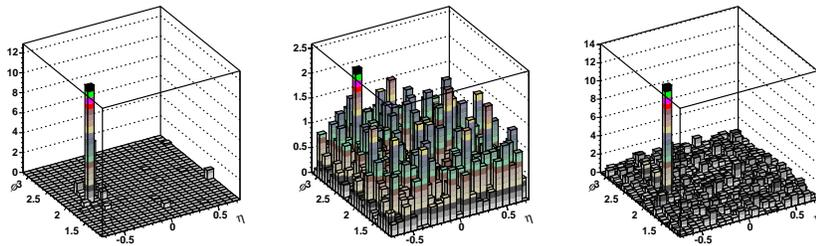


Figure 2: Energy distribution vs.  $\eta$  and  $\phi$  in EMCal acceptance. One cell corresponds to  $5 \times 5$  EMCal towers ( $\Delta\eta \times \Delta\phi \sim 0.070 \times 0.070$ ). Left: 55 GeV PYTHIA generated jet; center: HIJING event with  $b \sim 5$  fm.; right: superposition of the two events. Note variation of vertical scale.

The least-biased jet trigger in ALICE would combine the EMCal energy measurement with charged particle tracking in the High Level Trigger (HLT), which has input bandwidth  $\sim 15$  GB/s [7]. Taking into account the minbias data rate  $20 \text{ MB/evt} \times 4 \text{ kHz} \sim 80 \text{ GB/s}$ , a possible approach to jet triggering in Pb+Pb requires EMCal rejection of about a factor 10 at L1 (compatible with the maximum TPC gating rate of 1 kHz), with further rejection provided by the HLT using both EMCal and tracking detector measurements.

In this note we present the first exploratory studies of the L1 EMCal jet trigger performance for 5.5 TeV Pb+Pb collisions, using PYTHIA-generated jets, HIJING-generated background events [8] and a simple parameterized model of the EMCal response. We show that, within this model calculation, the required background rejection can be achieved while maintaining good efficiency for moderately high energy jets. Efficient and unbiased triggering may however be difficult to achieve in the intermediate  $E_T \approx 50$  GeV region, where the jet signal can be significantly distorted by background fluctuations.

## 2 EMCal response simulation

Particles generated by HIJING and PYTHIA are projected onto a two dimensional histogram representing the EMCal acceptance, with limits  $|\eta| < 0.7$  and  $\pi/3 < \phi < \pi$  and bin size  $\Delta\eta \times \Delta\phi = 0.014 \times 0.014$ . All strong, weak and electromagnetic decays occur at the primary vertex, located at the origin (i.e. no vertex smearing). Charged particle trajectories are bent in a uniform 0.5T field over the 4.6 m radial distance from the beamline to the EMCal front surface. Photons and electrons deposit 100% of their energy while hadrons deposit 25% [9]. The deposited energy is assigned to the tower onto which the track is projected, i.e. the spatial extent of the shower is ignored. Fig. 2 shows the EMCal response to a PYTHIA-generated 55 GeV jet, a background HIJING event with  $b \sim 5$  fm, and the superposition of the two.

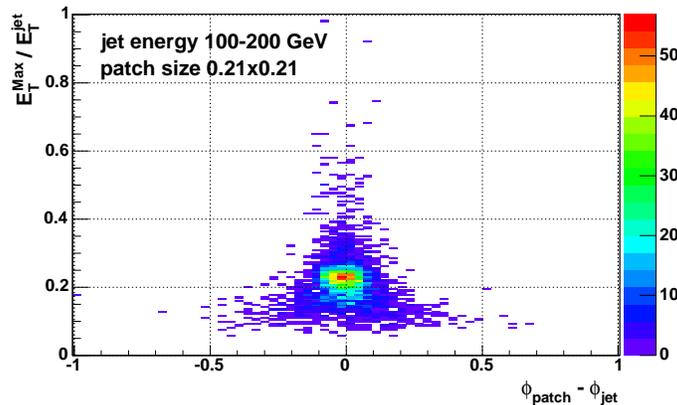


Figure 3: Comparison of L1 trigger algorithm and PYTHIA internal jet finder for PYTHIA events containing  $100 < E_T < 120$  jets and L1 patch size  $0.21 \times 0.21$ . Plot shows ratio of  $E_T$  vs. difference in angle for the two algorithms.

### 3 Level 1 jet trigger algorithm

The L1 jet trigger algorithm sweeps a square patch of dimensions  $\Delta\eta \times \Delta\phi$  over the EMCAL and finds the location of the patch with the highest integrated EMCAL energy ( $E_T^{\text{Max}}$ ). For computational efficiency the patch is moved in steps of size  $\Delta\eta/3$  and  $\Delta\phi/3$ , which generates negligible irresolution in  $E_T^{\text{Max}}$ . In this note we only consider jets that are nominally within the EMCAL acceptance, defined as jets whose centroid from the PYTHIA jet finder falls within the EMCAL excluding an boundary region of width 0.2 in both  $\eta$  and  $\phi$ .

Three patch sizes are considered in this note:  $\Delta\eta \times \Delta\phi = (0.14 \times 0.14)$ ,  $(0.21 \times 0.21)$ , and  $(0.35 \times 0.35)$ . CDF measurements of charged jet profiles in  $\bar{p} + p$  collisions show that for  $\sim 50$ -100 GeV jets about 80% of the jet energy is contained within  $R < 0.15$  [10], which sets the rough size scale for the core of the jet. Studies with isolated PYTHIA jets indicate that patch sizes as small as  $(0.05 \times 0.05)$  may have jet trigger efficiency comparable to that of larger patches [11]. However, such small patches are especially susceptible to variations in fragmentation, which is the physics we are after: the medium-induced modification of jets. A trigger should match as closely as possible the offline physics analysis algorithms that are applied to the datasets biased by it. We think it unlikely that the optimized jet algorithms for offline analysis will converge on jet definitions having  $R < 0.1$ . Our preferred strategy is rather to maximize the patch size in order to reduce trigger bias, though the size is limited from above by signal/background. We therefore do not consider patch sizes smaller than  $\sim 0.1 \times 0.1$  in this note.

### 4 Trigger response to PYTHIA-generated jets

Fig. 3 compares the response of the L1 trigger algorithm (trigger patch  $\Delta\eta \times \Delta\phi = 0.21 \times 0.21$ ) and the internal PYTHIA jet finder, for PYTHIA events

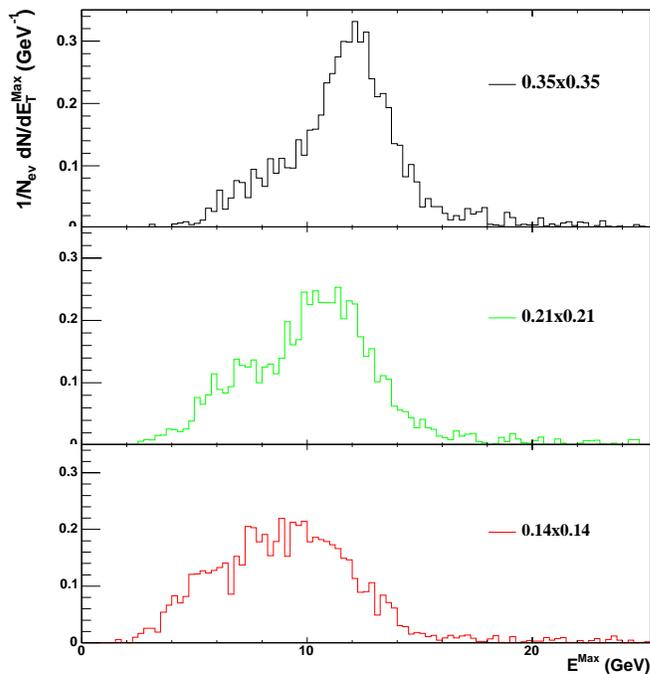


Figure 4: PYTHIA.  $E_T^{\text{Max}}$  for 50-60 GeV jets, different patch sizes as indicated.

containing jets with  $100 < E_T < 120$  GeV. The vertical axis shows the ratio of  $E_T^{\text{Max}}$  from the trigger to the total jet energy from the PYTHIA jet finder. The ratio peaks at 20-30%, as expected since the EMCAL is sensitive primarily to the EM fraction of the signal. The horizontal axis shows the difference in azimuthal angle between patch center and the jet centroid from the PYTHIA jet finder. The trigger appears to point correctly ( $\delta\phi < 0.1$ ) except for cases in which significantly less than 20% of the jet energy is found. We speculate that small energy fraction correlated with poor pointing resolution results from the combined effects of fluctuations in fragmentation and limited acceptance. Understanding of such acceptance effects requires detailed physics study and is beyond the scope of this note.

Fig. 4 shows the  $E_T^{\text{Max}}$  distribution for jet energy 50-60 GeV and for three different patch sizes. The relative fluctuations are smallest for the largest patch size, as expected. Fig. 5 shows the  $E_T^{\text{Max}}$  distribution for varying jet energy and fixed patch sizes  $0.21 \times 0.21$  and  $0.35 \times 0.35$ . The response is seen to be broad in all cases. Fig. 6 shows the distribution of jet cross section for various lower bounds on  $E_T^{\text{Max}}$ . Cutting harder than  $E_T^{\text{Max}} > 10$  GeV evidently generates significant trigger biases for  $E_T^{\text{jet}} > 100$  GeV.

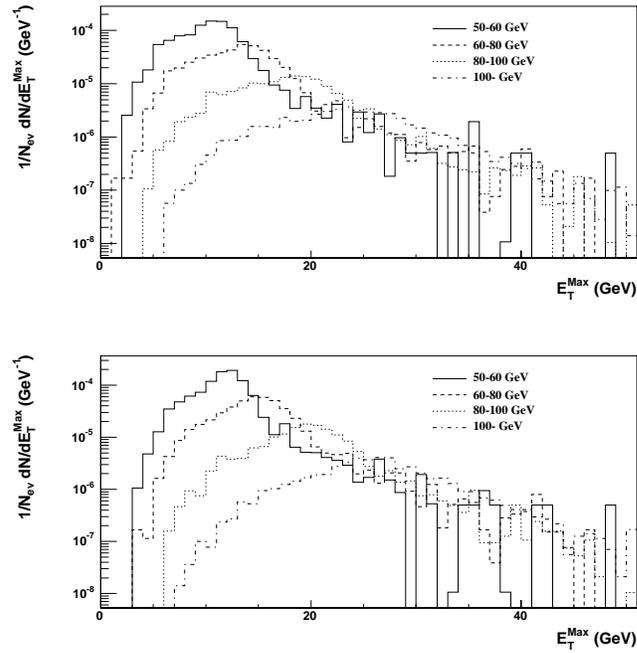


Figure 5: PYTHIA.  $E_T^{\text{Max}}$  distribution for different jet energies, for patches  $0.21 \times 0.21$  (upper) and  $0.35 \times 0.35$  (lower).

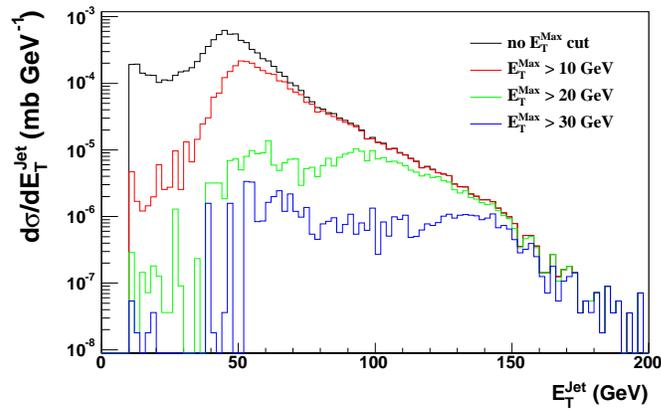


Figure 6: PYTHIA: trigger bias for various cuts on  $E_T^{\text{Max}}$ ; jet patch  $0.21 \times 0.21$ . Features at  $E_T < 50$  GeV are due to thresholds in event generation and should be disregarded.

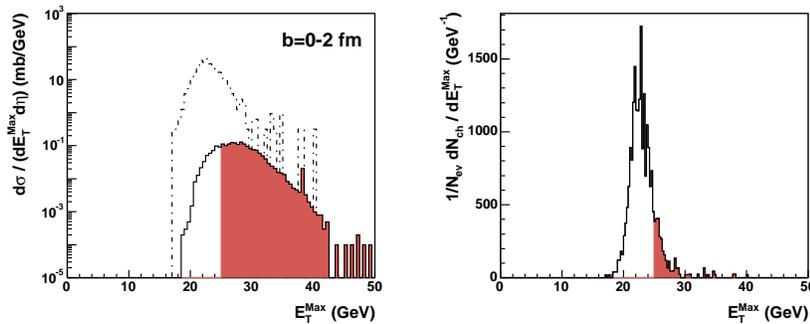


Figure 7: PYTHIA+HIJING,  $b=0-2$  fm (central collisions), jet patch  $0.21 \times 0.21$ . Left:  $E_T^{\text{Max}}$  differential cross section for background (dash-dot) and for background plus 50-60 GeV jets (solid). Filled area shows 80% of embedded jet yield. Right:  $E_T^{\text{Max}}$  distribution for the background events weighted by charged multiplicity in TPC, which is proportional to data volume. Filled area shows fraction of data volume that contains 80% of jet yield.

## 5 Trigger response to 50-60 GeV jets in Pb+Pb collisions

In this section we study the trigger response to PYTHIA jets embedded into HIJING events for 5.5 TeV Pb+Pb collisions. The presence of background fluctuations will contaminate the trigger response shown in the previous section for pure PYTHIA jets. We look in detail at the response of the trigger to 50-60 GeV jets, which turn out to be at the lower end of the triggerable jet spectrum in heavy ion events if background fluctuations are well described by HIJING.

Figs. 7 and 8, left panels, show the  $E_T^{\text{Max}}$  cross section (jet patch  $0.21 \times 0.21$ ) for central ( $b=0-2$  fm) and peripheral ( $b=8-10$  fm) Pb+Pb collisions and for the same events with 50-60 GeV jets superimposed. Cross-sections are calculated by taking into account the jet cross section from PYTHIA and the equivalent number of binary collisions for each event class.

The plots are generated using  $\sim 200$  PYTHIA-generated jets within the EM-Cal acceptance (PYTHIA jet finder) embedded into  $\sim 100$  HIJING events for each event class. We assume that this sample provides sufficient statistical variation to study the gross features of the trigger response addressed by this note. Since we require background data rate reduction of only a factor 10 or so, it is not necessary to simulate fully the background tail at high  $E_T^{\text{Max}}$  and thus large numbers of background events are not required.

The filled area in each figure shows 80% of the jet yield, i.e. its lower bound indicates the  $E_T^{\text{Max}}$  cut necessary for 80% jet efficiency. Background fluctuations are significant relative to the intrinsic fluctuations of the jet, both for central and for peripheral collisions. The overall level of background is seen to be strongly centrality-dependent, as expected, meaning that the  $E_T^{\text{Max}}$  threshold must vary with centrality for centrality-independent jet trigger efficiency.

The goal of the L1 jet trigger is to reduce the background *data rate* to match the HLT input bandwidth while maintaining good efficiency to accept

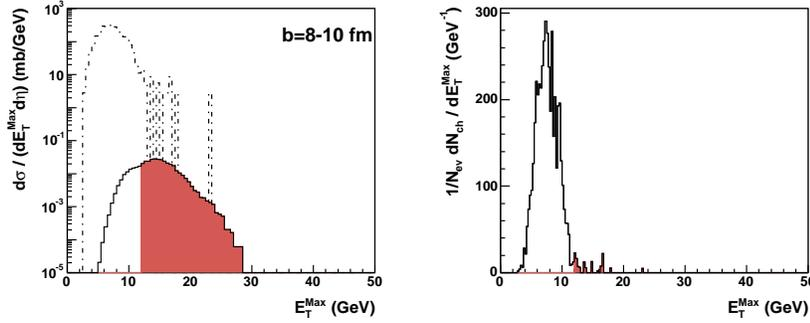


Figure 8: Same as Fig. 7 but for peripheral HIJING events with  $b=8-10$  fm.

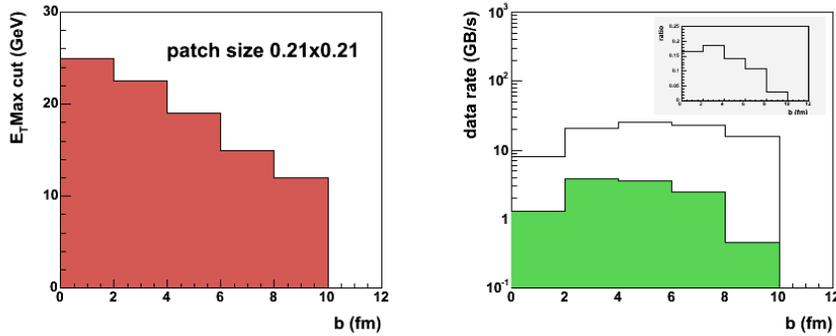


Figure 9: PYTHIA+HIJING, jet patch  $0.21 \times 0.21$ , jet  $E_T=50-60$  GeV. Left: impact parameter dependence of  $E_T^{\text{Max}}$  cut required for 80% jet efficiency. Right: impact parameter dependence of L1 input (upper histogram) and output (lower filled histogram) data rate using cuts in left panel. Insert shows their ratio.

events containing high  $p_T$  jets. We thus use reduction in data rate (in GB/s) rather than event rejection as the metric of the trigger rejection. The data rate is estimated using the TPC multiplicity, which dominates the ALICE event size [12]:

$$\text{event size [MB]} = 0.009 \times N_{\text{ch}} + 2.0,$$

where  $N_{\text{ch}}$  is the number of charged tracks in the TPC acceptance ( $|\eta| < 0.9$  and full azimuthal coverage). Figs. 7 and 8, right panels, show the  $N_{\text{ch}}$ -weighted distribution of  $E_T^{\text{Max}}$  for background events, with the filled area showing the fraction of the background data rate corresponding to 80% jet efficiency. Data rate is calculated using 4 kHz for minimum bias and taking into account the fraction of the minimum bias cross section containing each event class.

Fig. 9, left panel, shows the centrality dependence of the  $E_T^{\text{Max}}$  cut for a  $0.21 \times 0.21$  patch that is required to maintain 80% efficiency for 50-60 GeV jets. The right panel shows the centrality dependence of the L1 input and output data rates. We note in passing that, except for the most central collisions, the cross section and multiplicity offset each other and input data rate is to

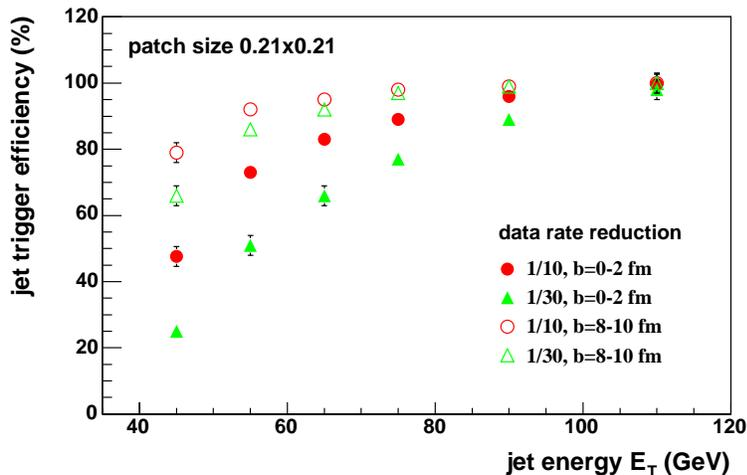


Figure 10: PYTHIA+HIJING: jet trigger efficiency as a function of jet energy for central and peripheral collisions, for a  $0.21 \times 0.21$  patch with data rate reduction of 1/10 and 1/30.

good approximation independent of centrality. The figure shows that, roughly speaking, a factor  $\sim 10$  reduction in data rate can be achieved while maintaining 80% trigger efficiency for moderate energy jets. This should be taken only as a qualitative indication that the required L1 performance is achievable. The specific numbers are dependent upon the models of signal and background, and the patch size and cuts have not been optimized. Better trigger efficiency will result if the relative background fluctuations are in reality smaller (as may be the case if there is strong jet quenching at the LHC), while poorer efficiency would result if medium-induced broadening transfers significant jet energy out of the patch.

## 6 Trigger efficiencies in Pb+Pb

We now discuss trigger efficiencies for Pb+Pb collisions more generally, determining the trigger efficiency for L1 data rate reduction of factors 10 and 30. This differs from the approach in the previous section, where the data rate reduction factor was determined to achieve fixed jet trigger efficiency of 80%.

Fig. 10 shows jet trigger efficiency vs. jet energy for the  $0.21 \times 0.21$  patch for central and peripheral collisions. Efficiency is poor below  $\sim 50$  GeV especially for central collisions, and the 1/30 reduction generates a large additional loss in efficiency over a broad range.

Fig. 11 shows jet trigger efficiency vs. centrality for the  $0.21 \times 0.21$  patch for two jet energies. For 100 GeV jets the efficiency is arbitrarily good, whereas for 50-60 GeV jets it varies strongly with data reduction factor and has a weak centrality dependence.

Fig. 12 shows jet trigger efficiency vs. jet energy for data rate reduction 1/10,

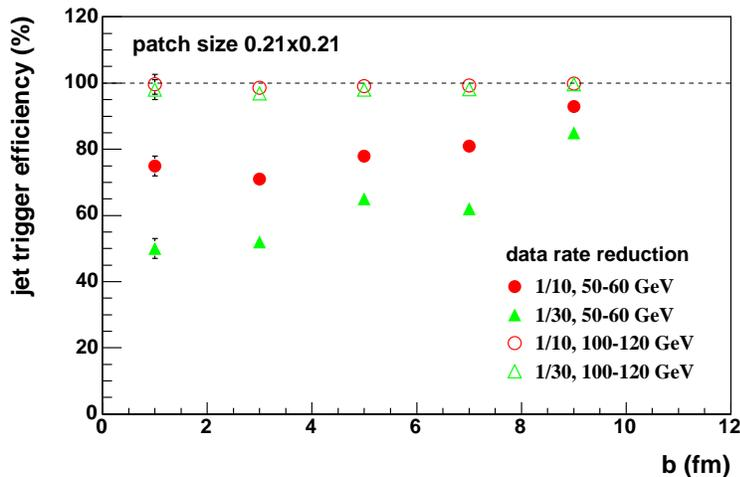


Figure 11: PYTHIA+HIJING: jet trigger efficiency as a function of impact parameter for two jet energies, for a  $0.21 \times 0.21$  patch with data rate reduction of 1/10 and 1/30.

for various patch sizes in central and peripheral collisions. There is no significant difference in performance between patches  $0.14 \times 0.14$  and  $0.21 \times 0.21$ , indicating that the gain in jet energy resolution for the latter relative to the former is offset by the increased contribution of background fluctuations. The  $0.3 \times 0.3$  patch has systematically lower efficiency at fixed data rate reduction factor, indicating that it is somewhat larger than optimum for the PYTHIA+HIJING model of signal+background. Jet quenching effects could both broaden the jet and lessen the background fluctuations, in which case the optimum would shift to larger patch sizes.

We assess the effects of jet quenching on the trigger efficiency using the Parton Quenching Model (PQM) by Lozides et al. [13, 14] and the event generator PYQUEN by Lokhtin et al. [15]. Fig. 13 shows trigger efficiency vs. energy for central collisions for the various fragmentation models and for various trigger patch sizes. The quenching models introduce large and model-dependent reductions in efficiency up to  $E_T \sim 100$  GeV, though with no large distinction between the  $0.14 \times 0.14$  and  $0.21 \times 0.21$  patches. PYQUEN is known to generate very broad fragmentation, generating correspondingly low trigger efficiencies relative to PQM. The response of the  $0.3 \times 0.3$  patch is uniformly worse than that of the smaller patches though with smaller differences between the quenching models, presumably due to the overall smaller signal/background.

The quenching models used in Fig. 13 are somewhat crude, with modification of the angular distribution of jet fragments that is not well motivated theoretically. The figure should only be regarded as a qualitative indication that quenching could have significant influence on the trigger efficiencies.

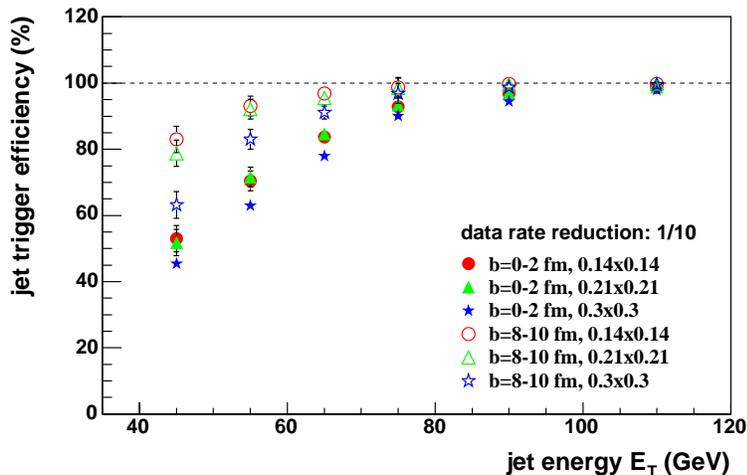


Figure 12: PYTHIA+HIJING: jet trigger efficiency vs. energy for 1/10 reduction in data rate, for various patch sizes and central and peripheral collisions.

## 7 Discussion

The calculations presented here are first, rough estimates of the L1 trigger performance of the EMCal. A number of improvements could be made in a straightforward way, including a more sophisticated model of EMCal response, simulation of the effects of intervening detector material, and a model of the trigger hardware architecture including granularity and digitization effects. However, we do not expect that such effects will alter qualitatively the results presented here.

A more serious limitation is due to the physics input to the simulations. While PYTHIA is a well calibrated model of vacuum jet fragmentation, HIJING is likely a poor estimate of background fluctuations. Most significantly, there are no Monte Carlo event generators available at present that incorporate theoretically well-motivated medium effects on the fragmentation of jets. Progress in this area is on the horizon through the incorporation of medium effects in the MLLA parton splitting functions [16, 17], which could lead to a PYTHIA-type event generator with a theoretically well controlled model of jet quenching.

Despite these uncertainties, some qualitative conclusions about EMCal trigger hardware design can be drawn from this study:

- The L1 rejection needed to match the HLT input bandwidth can likely be achieved while maintaining reasonable jet trigger efficiency over a broad energy range.
- Uniform jet trigger efficiency as a function of centrality in nuclear collisions requires a centrality-dependent trigger threshold. The centrality measurement should be supplied by an independent, azimuthally uniform device (the latter to avoid biases due to orientation of the reaction plane).

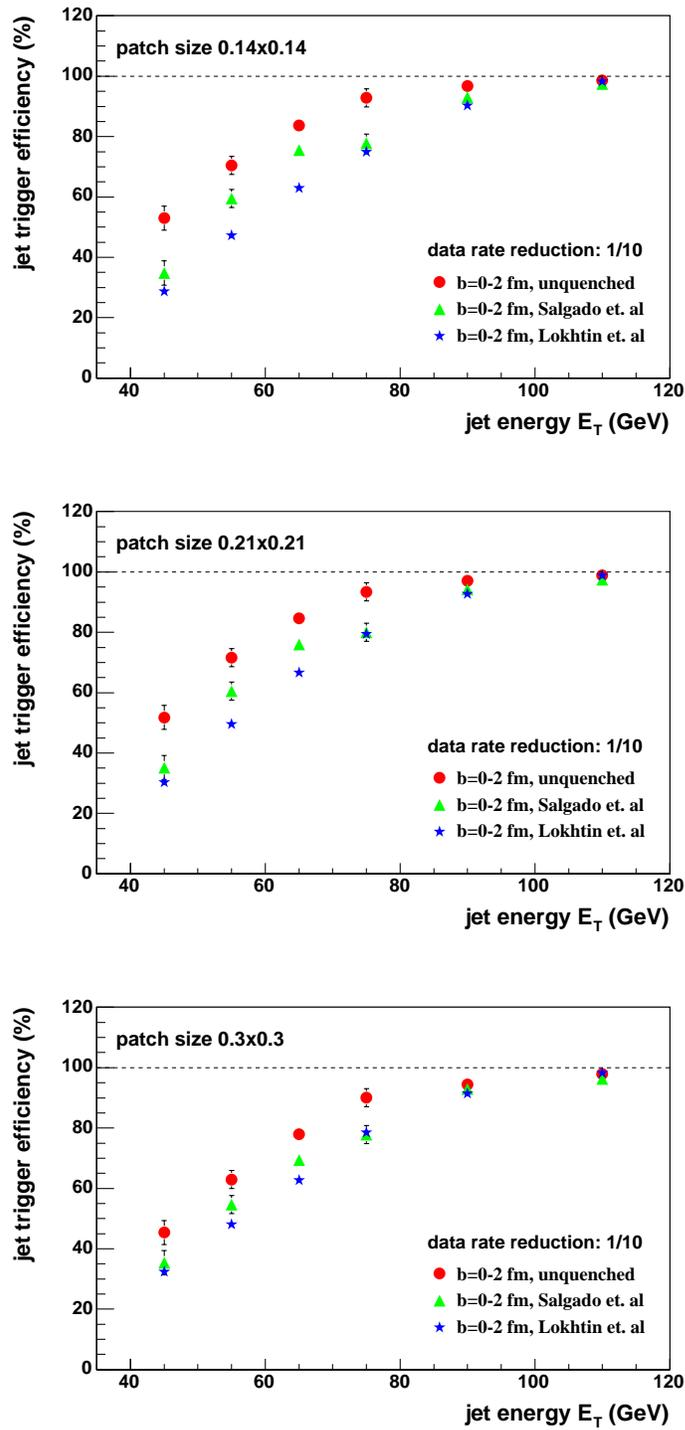


Figure 13: PYTHIA+HIJING+quenching: trigger efficiency vs. jet energy for central collisions for various jet quenching models and trigger patch sizes.

The V0 detector is the appropriate detector for this in ALICE, providing a signal proportional to multiplicity [18] on the required L1 timescale. Technical implementation is under discussion between the EMCal and V0 groups.

- Flexibility in jet trigger patch size: patch size is driven larger by the requirement of unbiased triggering in light of presently unknown and potentially large quenching effects, but is limited from above by increasing background for larger patch size. Optimization will only be possible once data come, but prudent hardware design should accommodate a range of patch sizes. The above calculations and general considerations of jet physics indicate that patch sizes beyond  $0.1 \times 0.1$  should be foreseen. Note that the PHOS TRU reads  $\sim 450$  towers, corresponding roughly to  $0.1 \times 0.1$ , so that the requirement to accommodate larger jet patch sizes implies the need to integrate  $E_T$  over multiple adjacent TRUs.

In addition to the above considerations for L1 triggering, integration of the EMCal into the High Level Trigger should also be looked into.

## References

- [1] P. Jacobs and X.-N. Wang, *Prog. Part. Nucl. Phys.* **54**, 443 (2005).
- [2] P. Jacobs, Status of EMCal project, Alice Club, May 9, 2005, [http://pjacobs.home.cern.ch/pjacobs/alice/EMCAL\\_ALICEclub\\_May05\\_final.ppt](http://pjacobs.home.cern.ch/pjacobs/alice/EMCAL_ALICEclub_May05_final.ppt).
- [3] C. Loizides, PhD thesis, Frankfurt/Main, 2005, nucl-ex/0501017.
- [4] A. Accardi *et al.*, CERN Yellow Report on "Hard Probes in Heavy Ion Collisions at the LHC: jet physics", hep-ph/0310274.
- [5] N. Carrer and A. Dianese, hep-ph/0311225.
- [6] F. Arleo *et al.*, CERN Yellow Report on "Photon Physics in Heavy Ion Collisions at the LHC", hep-ph/0311131.
- [7] ALICE Trigger, DAQ, HLT and Control System TDR; CERN/LHCC 2003-062.
- [8] Event generators: PYTHIA ver. 6.2.14; HLJING ver. 1.36.
- [9] STAR, J. Adams *et al.*, *Phys. Rev.* **C70**, 054907 (2004).
- [10] CDF, T. Affolder *et al.*, *Phys. Rev.* **D65**, 092002 (2002).
- [11] C. Anson, <http://pdsfweb01.nersc.gov/~canson/HijingHTMLStuff.html>.
- [12] ALICE PPR Volume I; CERN/LHCC 2003-049.
- [13] A. Dainese, C. Loizides, and G. Paic, *Eur. Phys. J.* **C38**, 461 (2005).
- [14] C. A. Salgado and U. A. Wiedemann, *Phys. Rev.* **D68**, 014008 (2003).
- [15] I. P. Lokhtin and A. M. Snigirev, *Eur. Phys. J* **C16**, 527 (2000), and hep-ph/0406038.

- [16] N. Borghini and U. Wiedemann, hep-ph/0506218.
- [17] X.-F. Guo and X.-N. Wang, Phys. Rev. Lett. **85**, 3591 (2000).
- [18] ALICE Forward Detector TDR; CERN/LHCC 2004-025.